670204

DP-MS-83-25

SIMULATION OF NATURAL CONVECTION IN A RECTANGULAR LOOP USING FINITE ELEMENTS

by

D. W. Pepper, L. L. Hamm, and A. B. Kehoe

E. I. du Pont de Nemours & Co.
Savannah River Laboratory
Aiken, South Carolina 29808

A paper proposed for presentation and publication
in the proceedings of the
Fifth International Conference on Finite Elements
and Flow Problems
Texas Institute for Computational Mechanics
The University of Texas at Austin
Austin, TX
January 23-26, 1984

This paper was prepared in connection with work done under Contract No. DE-AC09-76SR00001 with the U.S. Department of Energy.

SIMULATION OF NATURAL CONVECTION IN A RECTANGULAR LOOP USING FINITE ELEMENTS

D. W. Pepper, L. L. Hamm, and A. B. Kehoe*

Abstract

A two dimensional finite element analysis of natural convection in a rectangular loop is presented. A ψ-ω formulation of the Boussinesque approximation to the Navier-Stokes equation is solved by the false transient technique. Streamlines and isotherms at Ra = 10^4 are shown for three different modes of heating. The results indicate that corner effects should be considered when modeling flow patterns in thermosyphons.

Introduction

Natural convection in fluid loops has been studied by many investigators. Both theoretical and experimental analyses of the flow phenomena can be found in the literature for single and multiple loops; nearly all the studies assume one-dimensional flow. The purpose of this study is to examine the two-dimensional nature of the natural convection process in a simple rectangular loop. A numerical study is undertaken using finite element methodology to predict flow conditions. Extension of the work is underway to examine flow in a closed loop container used for cooling failed reactor assemblies at the Savannah River Plant (SRP), and thermosyphon cooling of the SRP nuclear reactors after shutdown.

Nearly all the early studies of natural convection in fluid loops involved heating the fluid from below, and cooling the fluid at the top of the loop.(1-4) Very little work has been conducted to examine theoretically the effects of heating a fluid loop along one vertical leg. In addition, corner effects have not been carefully examined for either heating case.

Governing Equations

In this study, a fluid loop is differentially heated and cooled in three separate modes as shown in Figures 1a, 1b, and 1c. The flow within the loop is assumed to be two dimensional. The nondimensional governing equations used to describe the flow and temperature within the loop are written in cartesian form as:(5,6)

$$\frac{Pr}{\alpha}\frac{\partial \omega}{\partial t} + \frac{\partial u\omega}{\partial x} + \frac{\partial v\omega}{\partial y} = Pr\nabla^2\omega + PrRa\frac{\partial \theta}{\partial x} \qquad (1)$$

* E. I. du Pont de Nemours & Co., Savannah River Laboratory, Aiken, South Carolina 29808

$$\frac{\partial \theta}{\partial t} + \frac{\partial u\theta}{\partial x} + \frac{\partial v\theta}{\partial y} = \nabla^2 \theta \qquad (2)$$

and

$$\frac{\partial \psi}{\partial t} = -\nabla^2 \psi - \omega \qquad (3)$$

where $u = \partial\psi/\partial y$, $v = -\partial\psi/\partial x$, ω is nondimensional vorticity, θ is the nondimensional temperature difference $(T-T_H)(T_H-T_c)$, and ψ is the nondimensional stream function. Use is made of the false transient technique.[5] Dirichlet and Neumann Boundary conditions associated with the equations are given by the general relation:

$$aG_s + h\frac{\partial G}{\partial n_s} - b = 0 \qquad (4)$$

where n_s denotes the coordinate normal to the surface, s, of the tube, and G is either stream function, vorticity or temperature; a and b are constants. The Prandtl number was set to 6.82, corresponding to water at 22 C.

Finite Element Method

The finite element method is chosen to approximate the spatial dependence of flow within the fluid loop. Eight noded quadratic isoparametric elements are used to discretize the fluid domain (Figure 1). Applying Galerkin's method of weighted residuals to the governing equations yields:

$$\frac{Pr}{\alpha} \overline{\overline{C}} \frac{d\underline{\omega}}{dt} + [\overline{\overline{A}}(\underline{\psi}) + Pr\overline{\overline{K}}]\, \underline{\omega} = PrRa\overline{\overline{B}}\underline{\theta} \qquad (5)$$

$$\overline{\overline{C}} \frac{d\underline{\theta}}{dt} + [\overline{\overline{A}}(\underline{\psi}) + \overline{\overline{K}}]\, \underline{\theta} = \underline{0} \qquad (6)$$

and

$$\overline{\overline{C}} \frac{d\underline{\psi}}{dt} + \overline{\overline{K}}\, \underline{\psi} = -\overline{\overline{C}}\, \underline{\omega} \qquad (7)$$

where the matrix members are integrals evaluated by a nine-point gaussian quadrature. A trapezoidal scheme is used to solve the temporal nature of the equations. The wall values for vorticity are solved in terms of the interior and wall nodal values of the stream function by

$$\omega_B = \frac{3(\psi_B - \psi_I)}{\ell^2} - \frac{\omega_I}{2} \qquad (8)$$

An average non-zero mass flux through the legs may result due to the lack of C_2 symmetry between the gravitational vector and the boundary conditions. Under C_2 symmetry conditions, small boundary perturbations may also trigger net flows of an oscillatory nature. Due to the possibility of such net flows, unknown a priori, special basis functions for the stream function are necessary.

The value of the stream function on the inner wall of the rectangular loop is set to zero. On the outer wall the stream function is spatially constant, but may vary in time. For those elements adjacent to the outer wall, special basis functions are used which force the stream function to be constant along the outer wall. The stream function topology collapses the outer wall to a single nodal point in computational space. This procedure delocalizes the standard basis functions and combines the elements adjacent to the outer wall to an equivalent global element.[9]

The above solution strategy employs $C^{(0)}$ basis functions which allow only weak boundary conditions for the stream function. By setting the stream function constant along a wall, continuity is maintained but a violation of the no-slip condition between nodal points occurs. For the range of Reynolds numbers investigated, slippage was small. Inter-elemental discontinuity of the velocity field representation was minimal.

Results

Steady state solutions of the transport equations were obtained at Ra = 10^4 for the three modes of heating. Oscillatory flow and flow reversal were not observed. Although the flow converged to steady state, continued long running of the model could conceivably produce a flow reversal trend. Further calculations using the steady state results are being conducted to determine if this condition eventually develops. All solutions were obtained within approximately 900 time steps with t = .01 and a residual convergence of 0.001. Residual convergence was calculated by the relation

$$\text{residual} \equiv \frac{|\Delta\omega|}{|\omega|} \tag{9}$$

where $|\,|$ represents a norm and Δ a time step.

Heating All Inside Walls

Tests were made to validate the model's floating scheme for the outer wall stream function value using concentrically horizontal cylinders with the inside cylinder heated and outside cylinder cooled. The isotherms and streamlines obtained were in agreement with those of Powe, et al.[7] In the case of the rectangular loop (Figure 1a), the sharp corners at the top and bottom of the inside surfaces affect the flow regime by acting as separation points. The flow is relatively smooth and free of ripples at Ra = 10^4. Figures 2a and 2b for stream lines and isotherms, respectively, illustrate the effect of sharp corners on the induced flow by natural convection. Calculations at Ra = 10^5 showed the flow to be approaching an instability condition, prior to becoming fully turbulent (and truly transitory in nature).

Heating the Bottom Leg, Cooling the Top Leg

For this case, the bottom leg was heated, the vertical legs insulated, and the top leg cooled (Figure 1b). All internal values were initially set to zero. Symmetrical thermal plumes developed since no natural (physical) perturbation exists to cause the flow to become asymmetric - as generally happens in laboratory experiments. A temperature anomaly was arbitrarily introduced along the bottom leg to cause the fluid to move up the right vertical leg. This perturbation allowed the fluid to develop and recirculate throughout the thermosyphon in a counterclockwise motion. As the flow approached steady state conditions, two recirculation zones developed. Cell strength grew as the Rayleigh number increased. The cells are shown in Figures 3a and 3c for Ra $=10^4$ and 10^5, respectively. The corresponding isotherms at Ra $= 10^4$ are shown in Figure 3b.

Heating a Vertical Leg, Cooling the Opposite Leg

In this last mode of heating, one vertical leg was heated, the opposite vertical leg cooled, and the top and bottom legs insulated (Figure 1c). As seen in Figures 4a and 4b for Ra $= 10^4$, the fluid recirculates around the loop in a counterclockwise motion. Two small counter-rotating cells developed in each vertical leg. Rather large boundary layers developed along the inner and outer walls in both vertical legs. An increased Rayleigh number resulted in an increase in cell strength and elongation of the cell within each thermally active leg. A steady state solution was not achieved for Ra $= 10^5$. Results were not considered to be physically realistic. The flow appeared to converge to steady state after several hundred time steps, then reversed direction and diverged. This behavior is felt to be due in part to the coarse discretization used near the boundaries. A laboratory model did show two small cells in roughly the same locations as predicted by the numerical model for Ra $= 10^4$.[8]

Conclusions

The transient equations of motion and temperature were solved using eight noded isoparametric quadrilaterals; 638 node points were used to discretize the solution domain. Steady state solutions were achieved within about 900 time steps (t = 0.01) using false transient terms and a residual criteria of 0.001 for Ra $= 10^4$. Oscillatory motion and flow reversals were not observed for Ra $= 10^5$, except for the case with heating from the side. Two dimensional flow (the occurrence of recirculating cells) developed in the vertical legs for all cases. Results indicate that corner effects should be considered when developing analytical models to predict flow patterns in thermosyphons containing sharp corners.

Acknowledgment

The information contained in this article was developed during the course of work under Contract No. DE-AC09-76SR00001 with the U.S. Department of Energy.

References

(1) Britt, T. E. and D. C. Wood, "Free Convection in a Partially Submerged Fluid Loop" presented at the 21st. National Heat Transfer Conference, Seattle, Washington, June 1983; ASME paper 83-HT-67.

(2) Chato, J. C. "Natural Convection Flows in Parallel-Channel Systems," J. Heat Transfer, November 1963, pp 339-345.

(3) Chen, K., "The Influence of Loop Configuration on Closed-Loop Thermosyphons" presented at the 1982 Winter Annual Meeting of the ASME, November 14 - November 20, 1982, Phoenix, AZ, ASME Paper 82-WA/HT-63

(4) Keller, J. B. "Periodic Oscillations in a Model of Thermal Convection", J. Fluid Mech., 26, 1966, pp 599-606.

(5) Mallinson, G. D., A. D. Graham, and G. De Vahl Davis, "Three-Dimensional Flow in a Closed Thermosyphon", J. Fluid Mech., 109, 1981, pp 259-275.

(6) Pepper, D. W. and R. E. Cooper, "Numerical Solution of Recirculating Flow by a Simple Finite Element Recursion Relation", Computers and Fluids, 8, 1980, pp 213-223.

(7) Powe, R. E., Carley, C. T., and Carruth, S. L., "A Numerical Solution for Natural Convection in Cylindrical Annuli," J. Heat Transfer, Transactions of ASME, 1971, pp. 210-220.

(8) Shadday, H. A., Thermosyphon Cooling in a Rectangular Loop, manuscript in preparation, E. I. du Pont de Nemours, Savannah River Laboratory; 1983.

(9) Thomasset, Francois, Implementation of Finite Element Methods For Navier-Stokes Equations, 1981 Springer-Verlag, New York, p. 128.

$C \equiv \theta = 0$
$H \equiv \theta = 1$

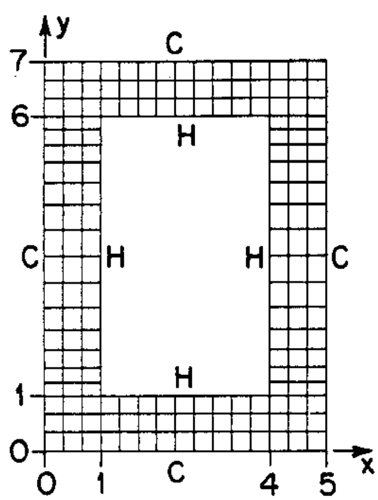

Figure 1a

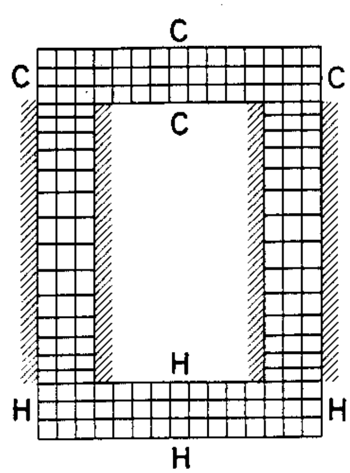

Figure 1b

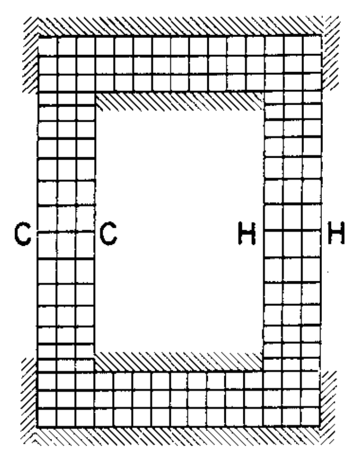

Figure 1c

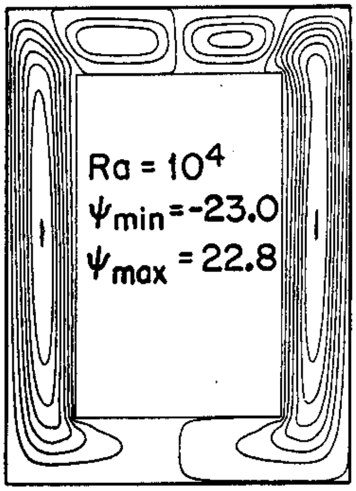

Figure 2a

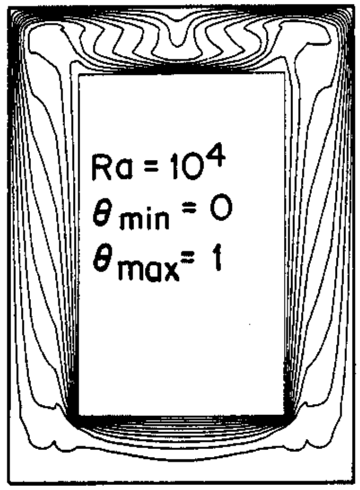

Figure 2b

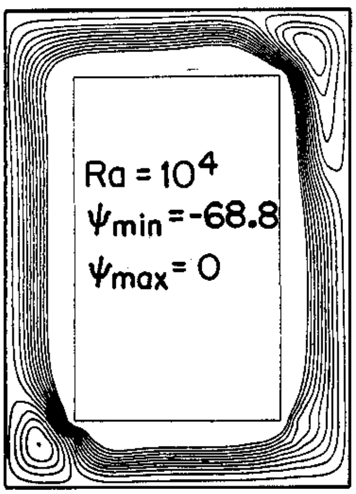

Figure 3a

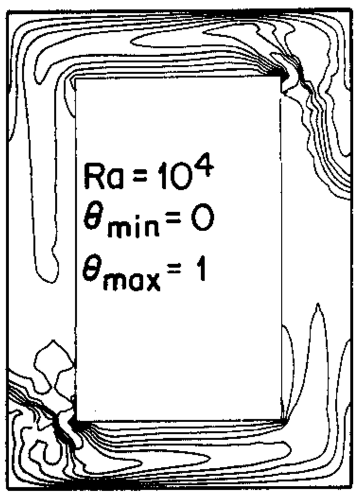

Figure 3b

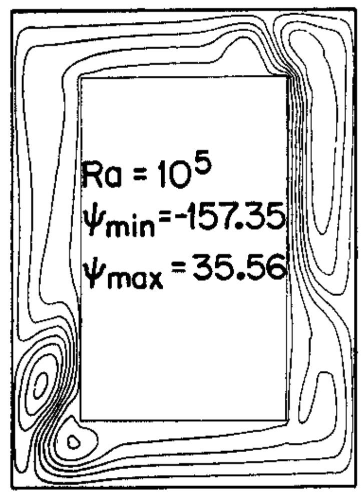

Figure 3c

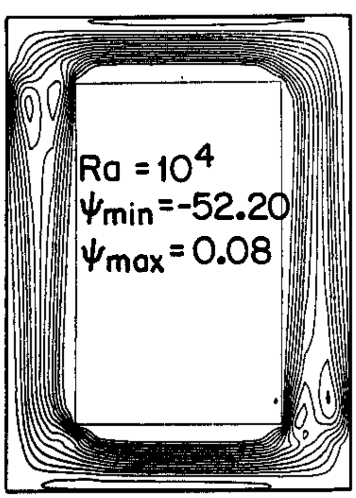

Figure 4a

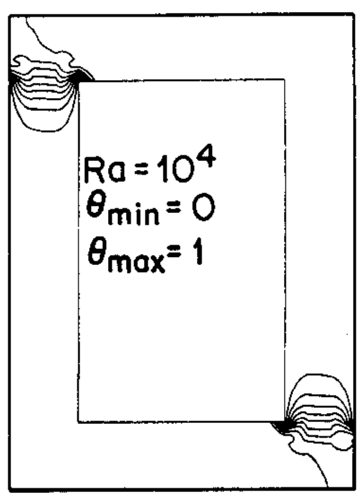

Figure 4b